ARTICLES

Magnetic Isotope Effect on Kinetic Parameters and Quantum Beats of Radical Pairs in Micellar Solution Studied by Optically Detected ESR Using Pulsed Microwave

Yasutaka Kitahama[†] and Yoshio Sakaguchi*

RIKEN (The Institute of Physical and Chemical Research), 351-0198 Wako, Saitama, Japan

Received: August 16, 2007; In Final Form: October 17, 2007

We investigated the quantum beats, the oscillation between singlet and triplet states of radical pairs induced by the microwave field resonant to one of the component radicals. They were observed as the alternation of the yields of the component radicals by a nanosecond time-resolved optical absorption with the X-band (9.15 GHz) resonant microwave pulse. This technique was applied to the photochemical reaction of benzophenone, benzophenone-d_{10}, and benzophenone-*carbonyl*-^{13}C in a sodium dodecylsulfate micellar solution with a step-by-step increase of the resonant microwave pulse width. The yields of the component radicals showed alternation with an increase of the microwave pulse width. This indicates that the radical pair retains spin coherence in the micellar solution. The magnetic isotope effect on the amplitude of the quantum beat was observed. The MW effect on the quantum beat of BP-^{13}C decreases from 80% to 60% of that of BP by irradiation of the π-pulse MW due to spin-locking. The kinetic parameters were also determined using the X- or Ku-band (17.44 GHz) region. They are almost similar to each other except for the intersystem recombination rate in the system of BP-^{13}C, which may be slightly higher than those in other systems.

Introduction

Chemical reactions through radical pairs (RPs) are affected by static and oscillating magnetic fields.[1,2] The former is known as the magnetic field effect (MFE), and the latter is called the reaction yield detected magnetic resonance (RYDMR). The geminate recombination of RPs proceeds from the singlet state (S). In the absence of a static magnetic field, all spin states of RPs, singlet and three triplet sublevels, are degenerated. The triplet states (T) induce S−T conversion and can recombine through S. In the presence of a static magnetic field, they split into three sublevels (T_{+1}, T_0, and T_{-1}). $T_{\pm1}$ states are separated from T_0 and S states by Zeeman splitting. Then only T_0 state is converted to the S state due to the degeneration and can recombine. The magnetic field suppresses S−$T_{\pm1,0}$ conversions and the geminate recombination. The resonant oscillating magnetic fields (microwave, MW), whose energy is equal to the Zeeman splitting, induce transition from the $T_{\pm1}$ to the T_0 state. Then, $T_{\pm1}$ states are also converted to S via the T_0 state and recombine. Thus the MW accelerates S−$T_{\pm1,0}$ conversions and the geminate recombination.

The S−$T_{\pm1,0}$ conversions are strongly influenced by hyperfine coupling (HFC) interactions. Therefore isotopic RPs which have different nuclear spins show distinctive spin dynamics. We refer to this phenomenon as the magnetic isotope effect (MIE).[3,4] For example, the lifetimes of the RPs formed by the photochemical reaction of benzophenone (BP), benzophenone-d_{10} (BP-d_{10}), and benzophenone-*carbonyl*-^{13}C (BP-^{13}C) in sodium dodecylsulfate (SDS) or polyoxyethylene dodecyl ether (Brij 35) micellar solution have been studied.[5−11] The MIEs could be explained by the HFC mechanism in a low magnetic field, 0−70 mT, and the relaxation mechanism in a high magnetic field, 0−30 T. The isotope enrichments and enhanced MIEs using the resonant MW have been illustrated experimentally.[12−14]

Recently, the RYDMR using a short MW pulse and a nanosecond time-resolved optical absorption have been applied to the studies on spin dynamics.[15−18] The pulse optical detected ESR (ODESR) can provide the optical signal in the absence and/or before the MW irradiation, which gives a reliable difference between the signal in the absence and presence of a MW pulse. If we use the MW detection, the signal in its absence can be obtained only at a limit of the power reduction. The low S/N ratio at this limit suffers the reliability of the signals. This is one of the major merits of ODESR over fast ESR techniques. We refer to the above difference as a "single pulse response", which shows the dynamic effect of the irradiated MW pulse. We can control many parameters of the MW irradiation such as the irradiation time, the pulse width, the pulse power, and so on, although the MW frequency is rather restricted owing to the resonance condition of the cavity. When we vary the MW irradiation time with reference to the reaction initiation fixing the other parameters, we get "pulse shift" data.[15−18] This extracts the dynamics of RPs from those of free radicals escaped from the pair which have the same optical absorption.

When we vary the MW pulse width fixing the other parameters, we get "pulse extension" data, which is similar to varying the MW power. In this experiment, we can control the rotating angle of the electron spin along the MW magnetic axis. Imagine a RP consisting of radicals a and b which has αα spins

* Corresponding author. E-mail: ysakaguc@riken.jp.
[†] Present address: Department of Chemistry, School of Science and Technology, Kwansei Gakuin University, Kobe-Sanda Campus, 2-1 Gakuen Sanda 669-1337, Japan.

10.1021/jp076611w CCC: $40.75
Published on Web 12/15/2007

(T_{+1} state). When we irradiate the MW field whose magnetic component is perpendicular to the external field, the α-spin on the radical a which is resonant to the MW starts to rotate and turns to a β-spin. Then the RP has $\alpha\beta$ spins (ST_0 mixed state) and can recombine. The β-spin rotates and returns to an α-spin by the elongated irradiation of the MW field. Then the RP recovers αα spins (T_{+1} state) again. It shows the periodic changes in the spin-state populations of the RP and is called the quantum beat.[19,20]

The oscillation frequency depends on the resonant MW field strength, $B_1 = \omega_1/\gamma_e$ (ω_1 is the Rabi frequency, and γ_e is the gyromagnetic ratio), and the difference of the resonant frequencies of the radicals a and b, $|\omega_a - \omega_b|$.[21]

A "weak" B_1 field ($\omega_1 \ll |\omega_a - \omega_b|$) induces the rotation between αα (or $\beta\beta$) and $\alpha\beta$ spins, namely, between $T_{\pm1}$ and ST_0 mixed states. Its oscillation frequency is ω_1. On the other hand, a "strong" B_1 field ($\omega_1 \gg |\omega_a - \omega_b|$) induces the rotation of both spins, that is, between αα and $\beta\beta$ spins via $\alpha\beta$ spins whose magnetic component is perpendicular to the external magnetic field. Namely, the rotation takes place within $T_{\pm1,0}$ states, and the geminate recombination is suppressed. This situation is called the spin-locking. The frequency of oscillation between $T_{\pm1}$ and T_0 states doubles, $2\omega_1$.

In this paper, we generated the RPs consisting of a BP ketyl radical (BPH•) and a SDS alkyl radical (•SDS), and we observed the yields of the escaping ketyl radical with changing MW pulse width in the condition of a "weak" B_1 field. The quantum beat in the system of 4,4′-difluorobenzophenone (F_2BP) which has large hyperfine anisotropy was compared with those of BP and its isotope derivatives. The kinetic parameters of the RPs were also determined by the optical detected X- (9.15 GHz) and Ku-band (17.44 GHz) ESR.

Experimental Section

Benzophenone (Cica-Merck) and 4,4′-difluorobenzophenone (Aldrich) were recrystallized from ethanol. Benzophenone-d_{10} (99 atom % D, Merck, Sharp & Dohme), benzophenone-*carbonyl*-^{13}C (99 atom % ^{13}C, ISOTEC), and sodium dodecylsulfate (Cica-Merck) were used as obtained. Distilled water for high-performance liquid chromatography (Cica-Merck) was purified in an Iwaki UP-100 ultrapure water system by ion-exchanging and ultrafine filtering. The sample solutions were degassed by blowing N_2 gas on the surface to avoid bubbling and flowed into a quartz tube at room temperature. The concentration of SDS and BPs were 0.08 and 0.002 mol dm^{-3}, respectively. The fourth harmonic, 266 nm, of an Nd:YAG laser (Quanta Ray GCR-3, Spectra-Physics) was used as an exciting light source. We observed the time profiles of the transient absorptions of their ketyl radicals at 525 nm for each compound. The measurement systems were similar to that described elsewhere.[15,18] The maximum MW fields for our X- and Ku-band apparatus were 1.6 and 0.36 mT, respectively.

Results and Discussion

ODESR Spectra.

Figure 1 shows the ODESR spectra of the RPs formed by hydrogen abstraction reactions of photoexcited BPs in SDS micellar solution. The X-band MW (9.15 GHz) was irradiated with $\Delta t_{MW} = 10$ μs, $t_D = -0.5$ μs, and $B_1 = 0.04$ mT. Here Δt_{MW} is the MW pulse width, t_D is the delay time to irradiate the MW pulse with reference to the laser excitation, and B_1 is the MW field estimated by the relation between the frequency of the quantum beat and the MW power. These spectra were observed as the decreases of the absorbance of their ketyl

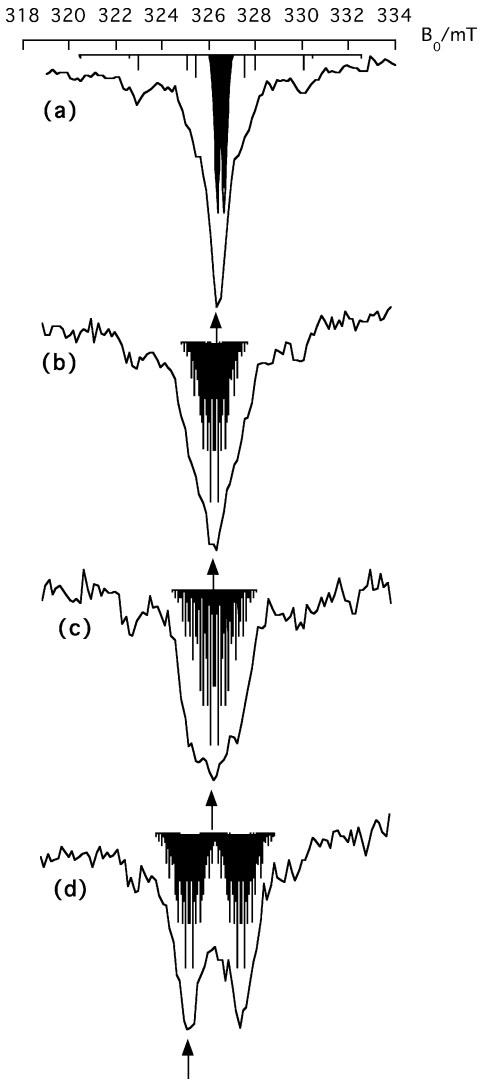

Figure 1. The ODESR spectra, which are measured as the absorbance of each BP ketyl radical averaged from 10 to 18 μs after the laser irradiation, observed by the photochemical reaction of (a) BP-d_{10}, (b) BP, (c) F_2BP, and (d) BP-^{13}C in SDS micellar solution. The stick diagrams of (a) SDS alkyl, BP-d_{10}, (b) BP, (c) F_2BP, and (d) BP-^{13}C ketyl radicals also are shown. The arrows show the resonance points where the quantum beats shown in Figure 5 and the data analysis shown in Table 1 and 2 are taken.

radicals, which were accelerated by the population transfer from the nonreactive $T_{\pm1}$ states to the reactive ST_0 mixed state by the resonant MW. The ODESR spectra in the system of BPH•-d_{10} and F_2BPH• were narrower and broader than that of BPH• because of the smaller HFC of deuterium and additional hyperfine splitting due to fluorine, respectively. For BPH•-^{13}C, the ODESR spectrum was split by the hyperfine splitting due to ^{13}C.

In this study, the dispersion of spin is the important parameter. In the absence of distinct HFC components, it is given by[19,21]

$$\Delta(\mathrm{a}) = \left[\frac{2}{3}\sum_i^{\mathrm{a}} a_i^2 I_i(I_i+1)\right]^{1/2} \quad (1)$$

where I_i is the nuclear spin quantum number of the ith nucleus in radical a, and a_i is its isotropic HFC constant. We estimated the values of Δ using the a_i values as follows: a(α-H) = 2.1

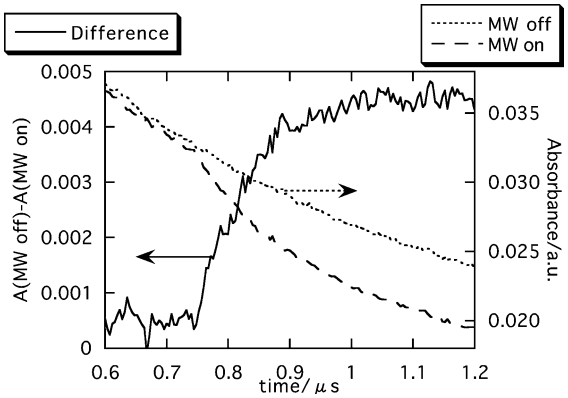

Figure 2. The difference of absorbance, $A(t)$, curves due to BP-^{13}C ketyl radical between in the absence and presence of the X-band resonant MW pulse which is shown by the solid line. The dotted (---) and broken (− −) lines show the $A(t)$ in the absence and presence of the microwave pulse, respectively.

mT, $a(\beta\text{-H}) = 2.5$ mT for •SDS;[22,23] $a(o\text{-D}) = 0.05$ mT, $a(m\text{-D}) = 0.02$ mT, $a(p\text{-D}) = 0.056$ mT, $a(\text{OH}) = 0.29$ mT for BPH•-d_{10};[22,23] $a(o\text{-H}) = 0.323$ mT, $a(m\text{-H}) = 0.123$ mT, $a(p\text{-H}) = 0.366$ mT, $a(\text{OH}) = 0.303$ mT for BPH•;[24] $a(p\text{-F}) = 0.75$ mT for F_2BPH•;[25] $a(^{13}\text{C}) = 2.2$ mT for BPH•-^{13}C.[26] The a(protons) of F_2BPH• and BPH•-^{13}C are assumed to be the same values to BPH•. The value of Δ(•SDS) is 3.8 mT. For the counter radicals, Δ(BPH•-d_{10}) = 0.36 mT, Δ(BPH•) = 0.65 mT, Δ(F_2BPH•) = 0.9 mT, and Δ(BPH•-^{13}C) = 1.7 mT. The observed line widths were 1.0, 2.4, 3.0, and 3.8 (=1.9 × 2) mT for the systems of BP-d_{10}, BP, F_2BP, and BP-^{13}C, respectively. This order agrees with that of the decrements induced by the MW, that is, the MW effect at a certain irradiation becomes smaller for the compounds with a wider spectrum. It is thought that if the condition $B_1 > \Delta(\text{a})$ is fulfilled, the MW rotates all spins on the radical a as single spin. Then the observed frequency of the quantum beat coincides with the Rabi frequency, $\omega_1 = \gamma_e B_1 = g\mu_B B_1 \hbar^{-1}$. When B_1 is larger than Δ(a) and Δ(b), the spin-locking effect occurs, and the frequency of the quantum beat becomes $2\omega_1$.

Determination of the Kinetic Parameters.

In the presence of an external magnetic field, the reaction scheme of photoexcited BP in a SDS micellar solution is described as follows:[27]

$$\text{BP} \rightarrow {}^1\text{BP}^* \rightarrow {}^3\text{BP}^* \tag{2}$$

$${}^3\text{BP}^* + \text{SDS} \xrightarrow{k_H} {}^{T_{\pm1,0}}(\text{BPH}^\bullet\ {}^\bullet\text{SDS}) \tag{3}$$

$${}^{T_0}(\text{BPH}^\bullet\ {}^\bullet\text{SDS}) \leftrightarrow {}^{S}(\text{BPH}^\bullet\ {}^\bullet\text{SDS}) \tag{4}$$

$${}^{T_{\pm1}}(\text{BPH}^\bullet\ {}^\bullet\text{SDS}) \xleftrightarrow{k_{Rlx}} {}^{S,T_0}(\text{BPH}^\bullet\ {}^\bullet\text{SDS}) \tag{5}$$

$${}^{S}(\text{BPH}^\bullet\ {}^\bullet\text{SDS}) \xrightarrow{k_{Rec}} \text{geminate recombination products} \tag{6}$$

$${}^{T_{\pm1,0}}(\text{BPH}^\bullet\ {}^\bullet\text{SDS}) \xrightarrow{k_{SOC}} \text{geminate recombination products} \tag{7}$$

$${}^{S,T_{\pm1,0}}(\text{BPH}^\bullet\ {}^\bullet\text{SDS}) \xrightarrow{k_{Esc}} \text{BPH}^\bullet + {}^\bullet\text{SDS} \tag{8}$$

Here eq 4 represents the S−T_0 mixing whose rate constant is larger than any other rate constants. The resonant MW induces the transition between the $T_{\pm1}$ states and the ST_0 mixed state. This process is formally the same as the acceleration of eq 5. From the data obtained by the X- and Ku-band ODESR using the short MW pulse, we determined the following kinetic parameters: eq 3: the hydrogen abstraction reaction rates, k_H; eq 5: the spin−lattice relaxation rates (without MW pulse), k_{Rlx}; eq 6: the recombination rates of the singlet RPs, k_{Rec}; eq 7: the intersystem recombination rates, k_{SOC}, which occur from triplet RPs due to the spin−orbit coupling; eq 8: the escape rates, k_{Esc}.

Figure 2 shows the time profiles of the transient absorptions due to the ketyl radicals, $A(t)$, in the absence and presence of a single short MW pulse and their difference, which is called "single pulse response". The X-band MW pulse was irradiated with $\Delta t_{MW} = 15$ ns, $t_D = 750$ ns, and $B_1 = 1.2$ mT. Because the populations of the $T_{\pm1}$ state are generally larger than those of the ST_0 mixed state due to much smaller k_{SOC} and k_{Rlx} than k_{Rec}, the resonant MW pulse transfers the RP in the $T_{\pm1}$ states to that in the ST_0 mixed state within Δt_{MW}. Since the decay of the ST_0 mixed state is much faster than those of the $T_{\pm1}$ states, the total population of RP after the MW pulse irradiation decreases faster than that in the absence of irradiation. If we use a very short MW pulse, the disappearance of the transferred population of RP due to the MW pulse cannot be completed within Δt_{MW}. Thus, we can obtain the decay rate of the ST_0 mixed state, $k_{dec} \approx k_{Rec}/2 + k_{SOC}/2 + k_{Esc} + k_{Rlx}$, by fitting the fast exponential decay part of the subtraction of the $A(t)$ in the absence and presence of the MW pulse as shown in Figure 2.

Figure 3 represents the decrements of the component radicals of RPs due to the MW pulse with "pulse shift technique", namely, shifting the irradiation time of the MW pulse with reference to the laser excitation, t_D. The MW pulses were irradiated with $\Delta t_{MW} = 15$ ns, $t_D = -0.5$ to 8 μs, $B_1 = 1.2$ (X-band) or 0.36 mT (Ku-band). The effect of MW pulse is proportional to the difference between the $T_{\pm1}$ states and the ST_0 mixed state, $[T_{\pm1}] - [ST_0]$. Since $[T_{\pm1}]$ and $[ST_0]$ grow together with the formation of RP via reaction, $[T_{\pm1}] - [ST_0]$ increases with k_H except for the special polarization that $[T_{\pm1}] = [ST_0]$. In the early stage after laser excitation, it can be assumed that only $[ST_0]$ decreases through the recombination with k_{dec}, which contributes to the increase of $[T_{\pm1}] - [ST_0]$. Therefore the rise of $[T_{\pm1}] - [ST_0]$ consists of two components, k_H and k_{dec}. On the other hand, the quasi-stationary concentration of ST_0 mixed state is very low at a later time due to the fast recombination. Therefore $[T_{\pm1}] - [ST_0]$ is almost equal to $[T_{\pm1}]$ at a later delay time, and hence its decay rate is determined by the decrease in $[T_{\pm1}]$. We estimated the values of k_H and the decay rates of the $T_{\pm1}$ states, $k_{T_{\pm1}} = k_{SOC} + k_{Esc} + k_{Rlx}$, by the fitting of the rise and decay of the curves as shown in Figure 3, respectively.

In Figure 3, the decay of the curves depends on the external magnetic field, which originates from the magnetic field dependence of the spin−lattice relaxation. Under high magnetic field, k_{Rlx} is proportional to B_0^{-2} in the absence of g anisotropy shown as

$$k_{Rlx} = \frac{\tau_c \gamma^2 {B_{loc}}^2}{1 + \tau_c^2 \gamma^2 {B_0}^2} \approx \frac{{B_{loc}}^2}{\tau_c {B_0}^2} \tag{9}$$

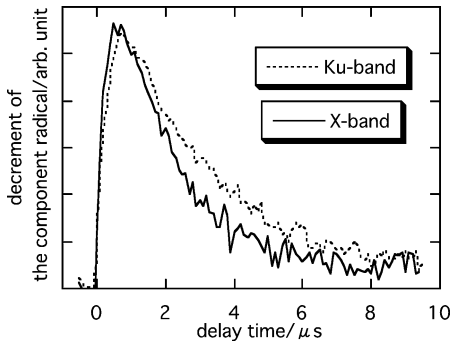

Figure 3. The difference between the yields of BP-^{13}C ketyl radical in the absence and presence of the resonant MW pulse. The signals were obtained by averaging $A(t)$ from 10 to 18 μs after the laser pulse and are plotted against the irradiation time of the resonant MW pulse with reference to the laser excitation, t_D. The curves are normalized to each other.

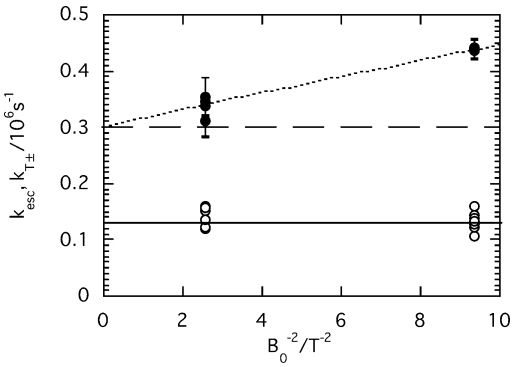

Figure 4. The external magnetic field dependence of the decay rates of the $T_{\pm1}$ states of radical pair formed from BP, $k_{T_{\pm1}}$ (closed circles). The escape rates, k_{Esc}, are given by open circles. The dotted (-----), broken ($-$ $-$), and solid lines show the values of $k_{Rlx} + k_{SOC} + k_{Esc}$, $k_{SOC} + k_{Esc}$, and k_{Esc}, respectively.

TABLE 1: Decay Rates of the ST_0 Mixed State (k_{dec}) and the $T_{\pm1}$ States ($k_{T_{\pm1}}$) at X-and Ku-band Regions (units are 10^6 s^{-1})

	k_{dec}(X-band)	$k_{T_{\pm1}}$ (X-band)	$k_{T_{\pm1}}$ (Ku-band)
BP	10 ± 1	0.44 ± 0.02	0.34 ± 0.03
BP-d_{10}	10 ± 1	0.44 ± 0.02	0.34 ± 0.04
BP-^{13}C	11 ± 1	0.52 ± 0.03	0.37 ± 0.05
F_2BP	10 ± 1	0.53 ± 0.03	0.34 ± 0.04

where τ_c is the rotational correlation time, γ is the electron gyromagnetic ratio, B_{loc} is the anisotropy of hyperfine coupling constants to induce the spin$-$lattice relaxation, and B_0 is the external magnetic field. The extrapolated value of $k_{T_{\pm1}}$ at $B_0^{-2} = 0$ is free from relaxation and equal to $k_{SOC} + k_{Esc}$. Then k_{Rlx} is derived from $k_{T_{\pm1}}(=k_{Rlx} + k_{SOC} + k_{Esc})$ and $k_{SOC} + k_{Esc}$. Here we estimate the contribution of g anisotropy in the spin relaxation. The relaxation rate due to g anisotropy is given by

$$k_{Rlx,\delta g} = \frac{(\tau_c \mu_B{}^2 \delta g^2 B_0{}^2)/5\hbar^2}{1 + \tau_c{}^2 \gamma^2 B_0{}^2} \qquad (10)$$

where μ_B and δg are Bohr magneton and g anisotropy, respectively. We calculated this rate using the parameters of $\tau_c = 16$ ps[10] and $\delta g = 0.0022$.[11] The $k_{Rlx,\delta g}$ at the X- and Ku-band regions are (6 and 11) $\times$ 10^3 s^{-1}, which are $\sim$5% and $\sim$25% of k_{Rlx} as shown in Figure 4 and Table 2, respectively. These values are within the errors of k_{Rlx}.

The escape rate, k_{Esc}, can be determined by the fitting of the difference between $A(t)$'s in the absence and presence of the external magnetic field,[17] which requires the exclusion of the transient absorptions due to the excited triplet states existing at similar wavelengths.[28] From k_{Esc} and $k_{SOC} + k_{Esc}$, the intersystem recombination rate, k_{SOC}, is derived. Thus the kinetic parameters, k_{SOC}, k_{Esc}, and k_{Rlx}, are determined as shown in Figure 4.[17] Furthermore, k_{Rec} is determined by k_{dec} ($\approx k_{Rec}/2 + k_{SOC}/2 + k_{Esc} + k_{Rlx}$), k_{SOC}, k_{Esc}, and k_{Rlx}.

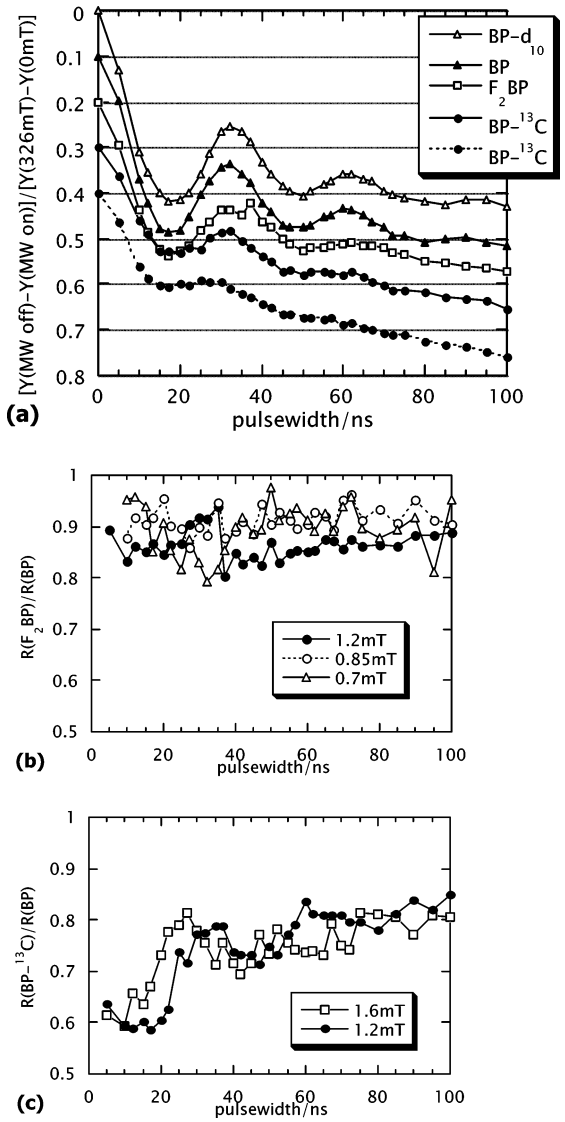

Figure 5. (a) Ratios of the decrements of the radical yields due to the resonant MW pulse (B_1 =1.2 mT) to the difference in the yields in the absence and presence of the external magnetic field of 326 mT. These MW effects are plotted against the MW pulse width. The yields of the radicals were averaged from 2.0 to 3.6 μs after the laser irradiation. Each curve is shifted relatively by 10%. The dotted curve shows the result of BP-^{13}C at the off-resonant point (326.5 mT). (b) Ratios of the MW effects in the system of F_2BP (open squares in (a)) to those of BP (closed triangles in (a)). These are plotted against the MW pulse width. (c) Ratios of MW effects in the system of BP-^{13}C (closed circles and solid lines in (a)) to those of BP (closed triangles in (a)). These are plotted against the MW pulse width.

Table 1 shows the observed decay rates of the ST_0 mixed and $T_{\pm1}$ states of the each RP. From these data and the above analyzing procedure, the kinetic parameters in Table 2 are determined. The distribution of the rate constants in Table 2 is strongly restrained to fulfill the B_0^{-2} dependence. It seems that k_{SOC} is too large compared to k_{Rlx} and k_{Esc}. The values in Table 2 should be read as a comparison within the derivatives. Each kinetic parameter is similar in all systems except for the

TABLE 2: Hydrogen Abstraction Reaction Rates (k_H), Recombination Rates of the Singlet RPs (k_{Rec}), Escape Rates (k_{Esc}), Intersystem Recombination Rates (k_{SOC}), Spin−Lattice Relaxation Rates (k_{Rlx}), and Decay Rates of the RPs in the Absence of the External Magnetic Field (k_0) (units are 10^6 s^{-1})

	k_H	k_{Rec}	k_{Esc}	k_{SOC}	k_{Rlx}(X-band)	k_{Rlx}(Ku-band)	k_0
BP	5 ± 2	19 ± 2	0.13 ± 0.02	0.17 ± 0.03	0.14 ± 0.02	0.04 ± 0.03	3.0 ± 0.8
BP-d_{10}	6 ± 2	19 ± 2	0.13 ± 0.02	0.17 ± 0.03	0.14 ± 0.02	0.04 ± 0.04	3.0 ± 0.8
BP-^{13}C	5 ± 2	20 ± 2	0.13 ± 0.02	0.19 ± 0.02	0.20 ± 0.04	0.05 ± 0.04	3.0 ± 0.8
F_2BP	6 ± 2	19 ± 2	0.12 ± 0.02	0.15 ± 0.02	0.26 ± 0.03	0.07 ± 0.04	3.0 ± 0.8

following two cases: (1) The relaxation of the RP consisting of F_2BPH• and •SDS is faster than those of the other RPs. It may be due to the large B_{loc}^2 of fluorine atoms. (2) The intersystem recombination rate in the system of BP-^{13}C may be slightly higher than those in other systems. The RP decay rates observed in SDS solution of BP-^{13}C up to 1 T have been higher than those of BP.[7] The MIE may be caused by larger k_{SOC}(BP-^{13}C) than k_{SOC}(BP). However, it has been reported that BPH•-^{13}C has large hyperfine anisotropy,[26] namely, large B_{loc}^2. If k_{SOC}(BP-^{13}C) is larger than k_{SOC}(BP), the MIE at ultrahigh magnetic fields can be observed. The MIEs up to 13 T have been investigated.[8,9] Notwithstanding, we cannot infer from these results that k_{SOC}(BP-^{13}C) is larger than k_{SOC}(BP) because of the large standard deviations of the RP lifetime data.

Isotope Effect on the Quantum Beat.

We observed the decrements of absorbance of BP ketyl radicals in the RPs by the irradiation of the MW pulse with "pulse extension", namely, step-by-step increase of the MW pulse width, Δt_{MW}. The X-band MW pulses (9.15 GHz) were irradiated with $\Delta t_{MW} = 0-100$ ns, $t_D = 750$ ns, and $B_1 = 1.2$ mT. The value of B_1 was larger than the dispersions of spins, Δ, except for BPH•-^{13}C. In Figure 5a, the ratios of the decrements of the yields of BP ketyl radicals due to the MW pulse to the difference in the yields in the presence and absence of the external magnetic field, [Y(MW off) − Y(MW on)]/[Y(326 mT) − Y(0 mT)] (the yield of the radical, Y, is average of the absorbance, $A(t)$, from 2.0 to 3.6 μs after the laser irradiation), are plotted with reference to the MW pulse width. Here the yields without the MW is equal to those in the presence of the external magnetic field, Y(MW off) = Y(326 mT). If the MW induces entire transition of the RP state between $T_{\pm1}$ and ST_0 mixed states (degeneration of $T_{\pm1,0}$ and S states), the state is same as RP in the absence of the external magnetic field. Therefore Y(MW on) ≥ Y(0 mT), and the ratio cannot become larger than 1. The ratios show MW effects more quantitatively than absolute values of the decrements, which are influenced by not only the MW but also the difference in the yields in the presence and absence of the external magnetic field.[17] The MW effects show periodic changes with reference to the pulse width. The MW induces transition of RP between $T_{\pm1}$ and ST_0 mixed states in the Rabi frequency, ω_1. The π-pulse MW ($\Delta t_{MW} = 1/2\omega_1$) transfers RPs from $T_{\pm1}$ to the reactive ST_0 mixed state. However, RPs return to the nonreactive $T_{\pm1}$ state via the ST_0 mixed state by the 2π-pulse MW ($\Delta t_{MW} = 1/\omega_1$). It is called the quantum beat. The quantum beats in the systems of BP-d_{10}, BP, and F_2BP oscillated in the Rabi frequency, $\omega_1 = \gamma_e B_1 = (30\ \text{ns})^{-1}$. In the system of BP-^{13}C at the resonant point (325.5 mT), the frequency also was similar to the Rabi frequency in spite of $B_1 < \Delta$(BPH•-^{13}C) = 1.7 mT. Unfortunately, we could not observe the quantum beat with B_1 larger than 1.7 mT. The quantum beat in the system of BP-^{13}C at the off-resonant point (326.5 mT) was too weak to discuss its frequency.

It is noteworthy that the amplitudes of the quantum beat in the system of BP-^{13}C and F_2BP were smaller than those of BP and BP-d_{10}. Figure 5, parts b and c, shows the ratios of the MW effects in the system of F_2BP and BP-^{13}C to those of BP, respectively. The MW effects for F_2BP system relative to those for BP system were about 0.9 and independent of Δt_{MW} up to 100 ns. The same trends were shown with a smaller MW field, $B_1 = 0.7$ and 0.85 mT, which are smaller than $\Delta(F_2\text{BPH}\bullet) = 0.9$ mT. In the system of BP-^{13}C, its MW effect relative to those for the BP system showed the minimum, maximum, and second minimum values (0.6, 0.8, and 0.7) by the irradiation of the π-, 2π-, and 3π-pulse ($\Delta t_{MW} = 15$, 30, and 45 ns at $B_1 = 1.2$ mT; $\Delta t_{MW} = 12$, 25, and 40 ns at $B_1 = 1.6$ mT), respectively. Then the ratios reached the constant about 0.8 by the longer pulse than the 3π-pulse. They were damped while oscillating in the Rabi frequencies.

It was shown that the decay of the quantum beat can be described using S−T dephasing caused by random fluctuation of electron exchange interaction (J) between the radicals[29] and T−T dephasing that originated in the random modulation of an electron spin dipole−dipole and an anisotropic hyperfine interaction.[20] It is thought that the interaction depends on the inter-radical distance and diffusional rotation. However, the J and the diffusion of the isotope derivatives may be almost the same among BP derivatives. In order to estimate the amount of J, we observed the time-resolved ESR spectra of the spin-correlated RP (SCRP) consisting of BP isotope ketyl radicals and SDS alkyl radical. In the SCRP, the hyperfine line splits emission/absorption (E/A) or A/E type peak by $2J$. The splitting of the outside lines due to •SDS in the SCRP spectra among the isotope derivatives at 750 ns after the laser excitation had similar values, which correspond to $2J = -0.32 \pm 0.04$ mT. Furthermore, the escape and recombination rates have similar values in all systems as shown in Table 2. These relate with the re-encounter frequency in the SDS micelle which may affect the dephasing. Therefore the quantum beat for BP-^{13}C may be characterized by the inefficient π-pulse MW effect rather than the fast dephasing.

We tried a simple quantum mechanical calculation that treats simply two independent spins having a coherent character at their birth.[21] There are no spin relaxations, chemical reactions, and interactions between two spins. The spin Hamiltonian in the rotating frame with the angular frequency of the MW field, ω, is given by

$$\mathcal{H} = (\omega_a - \omega)S_{az} + \omega_{1a}S_{ax} + (\omega_b - \omega)S_{bz} + \omega_{1b}S_{bx} \qquad (11)$$

where

$$\omega_a = g_a\mu_B B_0\hbar^{-1} + \sum_i a_i M_i,\ \omega_{1a} = g_a\mu_B B_1\hbar^{-1}$$

$$\omega_b = g_b\mu_B B_0\hbar^{-1} + \sum_j a_j M_j,\ \omega_{1b} = g_b\mu_B B_1\hbar^{-1} \qquad (12)$$

where M_i is the nuclear magnetic quantum number of the ith nuclei. The probability of finding the ST_0 mixed state for the initial T_{+1} state is

$$P_{ST_0}(t) = |\langle S|\exp(-i\mathscr{H}t)|T_{+1}\rangle|^2 + |\langle T_0|\exp(-i\mathscr{H}t)|T_{+1}\rangle|^2 \quad (13)$$

Equation 11 has been expressed by the analytical formula.[21] We considered the RPs forming radical a which has 10 hyperfine lines with an intensity ratio of 1:1:4:4:6:6:4:4:1:1 ($\Sigma a_i M_i$ = 6.05, 3.95, 3.55, 1.45, 1.05, −1.05, −1.45, −3.55, −3.95, −6.05 mT, respectively) corresponding to •SDS and radical b which has 1 ($\Sigma a_j M_j$ = 0 mT), 2 ($\Sigma a_j M_j$ = 1.1 and −1.1 mT), or 3 ($\Sigma a_j M_j$ = 0.75, 0, −0.75 mT), hyperfine lines corresponding to BPH•, BPH•-^{13}C, or F_2BPH•, respectively. The *g* values of radicals a and b are 2.003. The frequency of the MW field is 9.15 GHz. The external magnetic field is 326.5 mT except for the BP-^{13}C system (325.5 mT). The B_1 field of MW is 1.2 mT.

Figure 6a shows the calculated time profiles of the populations of the ST_0 mixed state for the initial T_{+1} state. The order of the calculated amplitude of the quantum beats within the 2π-pulse MW width, 30 ns, is BP > F_2BP > BP-^{13}C. Since we neglected the spin relaxation such as the T−T and S−T dephasing,[20,29] the calculated quantum beats do not decay.

Figure 6b expresses the calculated results in the cases of the center hyperfine line (—) and the sum of two side hyperfine lines (---) for F_2BPH•. The MW produces resonance at the center hyperfine line, but does not cause resonance at the side hyperfine lines. Therefore the dotted curve has a smaller amplitude and oscillates in a higher frequency than the solid curve which oscillates in the Rabi frequency, ω_1. In the case of resonant condition, the spin rotates on the axis which is perpendicular to the external magnetic field. When the off-resonant MW irradiates, the axis inclines to the external magnetic field and the spin. Then the spin runs along a smaller circle than that for the resonant condition. The precession frequency due to the off-resonant MW for the two spins is mainly determined by $\{\omega_1^2 + (\omega_b - \omega)^2\}^{1/2}$.[21]

In the system of BP-^{13}C, the calculated quantum beat was broken down into four cases according to whether the hyperfine lines of •SDS exist in the low- or high-field side ($\Sigma a_i M_i$ > 0 or $\Sigma a_i M_i$ < 0, respectively) and whether M_I of ^{13}C is +1/2 or −1/2 ($\Sigma a_j M_j$ = 1.1 or −1.1 mT, respectively). Here M_I is the nuclear spin magnetic quantum number. The results are shown in Figure 6c and as follows. (1) For the high-field side and M_I = +1/2 (—○—), the MW rotates the M_I = +1/2 spin of BPH•-^{13}C between the α and β spin. The RP changes between T_{+1} (αα) state and ST_0 mixed (αβ) state. Thus the frequency of the nutation coincides with ω_1. The amplitude is the largest in four cases. (2) For the low-field side and M_I = −1/2 (---●---), the beat oscillates in ω_1 because the partial hyperfine lines of •SDS in the low-field side resonate with the MW. (3) For the high-field side and M_I = −1/2 (---○---), the precession frequency due to the off-resonant MW for the two spins is mainly determined by $\{\omega_1^2 + (\omega_b - \omega)^2\}^{1/2}$,[21] which is accidentally similar to 2ω_1. The amplitude is the smallest in four cases. (4) For the low-field side and M_I = +1/2 (—●—), the spin-locking effect occurs because the condition $\omega_1 \gg |\omega_a - \omega_b|$ is partly fulfilled, where ω_a and ω_b are the resonant frequencies of the hyperfine lines of •SDS in the low-field side and the M_I = +1/2 spin of BPH•-^{13}C, respectively. Namely the MW rotates both spins partly. The beat oscillates in double the Rabi frequency, 2ω_1. From these results, especially case (4), we concluded that the π-pulse MW effect in the system of BP-^{13}C is always canceled out by the spin-locking effect as shown in Figure 5c.

Conclusion

In the systems of BP isotopes, each kinetic parameter is almost similar except for the case in which k_{SOC}(BP-^{13}C) may be slightly higher than k_{SOC}(BP) and k_{SOC}(BP-d_{10}). In the quantum beat, it is observed that the MW effect for BP-^{13}C decreases from 80% to 60% of that for BP by irradiation of the π-pulse. The reasons are not only inefficient spin-inversion due to the off-resonant MW for the RPs but also that the spin-locking effect partly takes place. For BP-^{13}C, the π-pulse MW effect is always smaller than the normal MW effects. There may be a probability that the enhanced magnetic isotope effects using the π-pulse MW in consideration of the quantum beat frequency are applied to isotope enrichment.

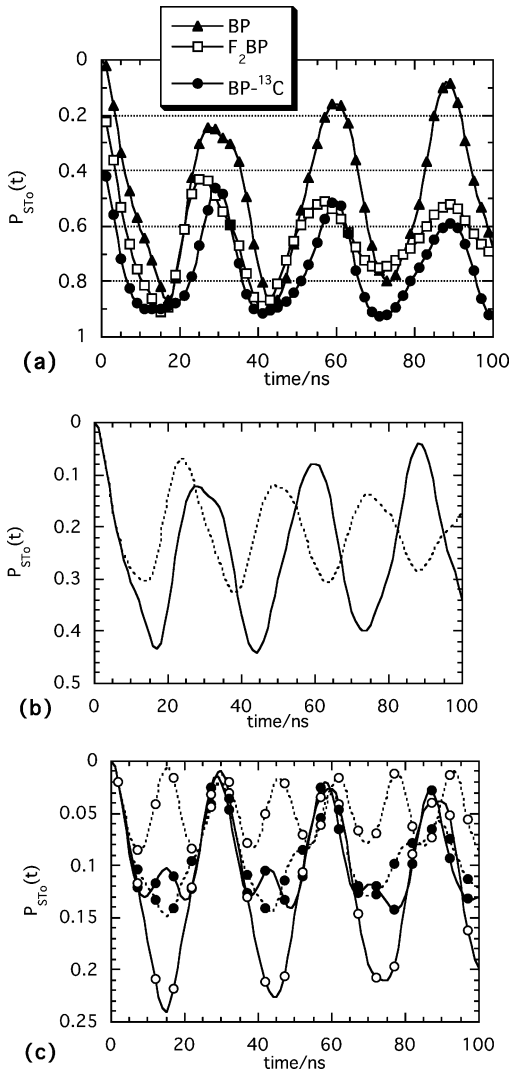

Figure 6. (a) The calculated time profiles of the probabilities of finding the ST_0 mixed state for the initial T_{+1} state under continuous resonant MW with B_1 = 1.2 mT. Each curve is shifted relatively by 20%. (b) The calculated time profiles of the probabilities of finding the ST_0 mixed state for center and side hyperfine lines of the F_2BP ketyl radical. Solid and dotted lines show the cases of the center hyperfine line and the sum of two side hyperfine lines due to the HFC of fluorine atoms, respectively. (c) The calculated time profiles of the probabilities of finding the ST_0 mixed state for four combinations of hyperfine lines of SDS alkyl and BP-^{13}C ketyl radicals. Closed and open circles show the cases in which the hyperfine lines of the SDS alkyl radical exist in the low- and high-field side, respectively. Solid and dotted lines show the cases of M_I = +1/2 and −1/2 due to the ^{13}C atom, respectively. Here M_I is the nuclear spin magnetic quantum number.

Acknowledgment. This work has been carried out under the MR Science Project and Special Postdoctoral Researchers Program of RIKEN. The authors are greatly indebted to Dr. Hisaharu Hayashi, Head of the Molecular Photochemistry Laboratory in RIKEN, for his continuing encouragement.

References and Notes

(1) Steiner, U. E.; Ulrich, T. *Chem. Rev.* **1989**, *89*, 51.
(2) Hayashi, H. *Photochemistry and Photophysics*, Vol. 1; CRC Press: Boca Raton, FL, 1990; p 59.
(3) Buchachenko, A. L. *Chem. Rev.* **1995**, *95*, 2507.
(4) Buchachenko, A. L. *J. Phys. Chem.* **2001**, *105*, 9995.
(5) Sakaguchi, Y.; Nagakura, S.; Minoh, A.; Hayashi, H. *Chem. Phys. Lett.* **1981**, *82*, 213.
(6) Sakaguchi, Y.; Hayashi, H.; Nagakura, S. *J. Phys. Chem.* **1982**, *86*, 3177.
(7) Hayashi, H.; Nagakura, S. *Bull. Chem. Soc. Jpn.* **1984**, *57*, 322.
(8) Fujiwara, Y.; Yoda, K.; Aoki, T.; Tanimoto, Y. *Chem. Lett.* **1997**, 435.
(9) Fujiwara, Y.; Taga, Y.; Tomonari, T.; Akimoto, Y.; Aoki, T.; Tanimoto, Y. *Bull. Chem. Soc. Jpn.* **200**, *174*, 237.
(10) Fujiwara, Y.; Mukai, M.; Tamura, T.; Tanimoto, Y. *Chem. Phys. Lett.* **1993**, *213*, 89.
(11) Nishizawa, K.; Sakaguchi, Y.; Abe, H.; Kido, G.; Hayashi, H. *Mol. Phys.* **2002**, *100*, 1137.
(12) Okazaki, M.; Shiga, T.; Sakata, S.; Konaka, R.; Toriyama, K. *J. Phys. Chem.* **1988**, *92*, 1402.
(13) Okazaki, M.; Toriyama, K. *J. Phys. Chem.* **1995**, *99*, 489.
(14) Tarasov, V. F.; Bagryanskaya, E. G.; Grishin, Y. A.; Sagdeev, R. Z.; Buchachenko, A. L. *Mendeleev Commun.* **1991**, 85.
(15) Sakaguchi, Y.; Astashkin, A. V.; Tadjikov, B. M. *Chem. Phys. Lett.* **1997**, *280*, 481.
(16) Woodward, J. R.; Sakaguchi, Y. *J. Phys. Chem. A* **2001**, *105*, 4010.
(17) Kitahama, Y.; Sakaguchi, Y. *Mol. Phys.* **2002**, *100*, 1451.
(18) Sakaguchi, Y. *Mol. Phys.* **2002**, *100*, 1129.
(19) Tadjikov, B. M.; Astashkin, A. V.; Sakaguchi, Y. *Chem. Phys. Lett.* **1998**, *283*, 179.
(20) Gorelik, V. R.; Maeda, K.; Yashiro, H.; Murai, H. *J. Phys. Chem. A* **2001**, *105*, 8011.
(21) Salikhov, K. M.; Molin, Y. N. *J. Phys. Chem.* **1993**, *97*, 13259. The equation (42) is misprinted.
(22) Closs, G. L.; Forbes, M. D. E.; Norris, J. R., Jr. *J. Phys. Chem.* **1987**, *91*, 3592.
(23) *Landolt-Bornstein Numerical Data and Functional Relationships in Science and Technology New Series Group II*; Vol. 9(b), pp 1−105 and 643.
(24) Wilson, R. *J. Chem. Soc. B* **1968**, 84.
(25) To the best of our knowledge, the value of a(*p*-F) for $F_2BPH\bullet$ has not been reported. Then we assumed the value is equal to a(*p*-F) for F_2BP anion radical as shown in *Landolt-Bornstein Numerical Data and Functional Relationships in Science and Technology New Series Group II*; Vol. 9(b), p 657.
(26) Murai, H.; Jinguji, M.; Obi, K. *J. Phys. Chem.* **1976**, *80*, 429.
(27) Sakaguchi, Y.; Nagakura, S.; Hayashi, H. *Chem. Phys. Lett.* **1980**, *72*, 420.
(28) Godfrey, T. S.; Hilpern, J. W.; Porter, G. *Chem. Phys. Lett.* **1967**, *1*, 490.
(29) Shushin, A. I. *Chem. Phys. Lett.* **1991**, *181*, 274.